2026

Analysis of CO2 adsorption in polymer-MOF compounds

BOSTON UNIVERSITY

COLLEGE OF ENGINEERING

Thesis

ANALYSIS OF CO_2 ADSORPTION IN POLYMER-MOF COMPOUNDS

by

ALEXANDER WALTER GUTHMANN

B.A., University of San Diego, 2021

Submitted in partial fulfillment of the

requirements for the degree of

Master of Science

2026

Approved by

First Reader

Sean Lubner, PhD
Assistant Professor of Mechanical Engineering
Assistant Professor of Materials Science and Engineering

Second Reader

Jörg G. Werner, PhD
Assistant Professor of Mechanical Engineering
Assistant Professor of Materials Science and Engineering

ANALYSIS OF CO_2 ADSORPTION

IN POLYMER-MOF COMPOUNDS

ALEXANDER WALTER GUTHMANN

ABSTRACT

Despite a drastic increase in resources dedicated to the study of metal-organic frameworks (MOF) in recent years, MOFs utilized for direct air capture (DAC) of CO_2 are still considered to be inefficient at large scale atmospheric CO_2 removal. To date, less than 10% of papers published on MOFs used for CO_2 capture focus on DAC applications [1]. Studies of MOF performance in simulated real-world environments are even more sparse in academic literature. In this thesis the effects of polystyrene binder additives on the CO_2 adsorption capacities of amine appended Mg_2(dobpdc) are analyzed experimentally with the goal of developing an optimized MOF coating that will improve efficiency and longevity in existing DAC technologies. The total CO_2 adsorption capacity of tetraamine appended Mg_2(dobpdc) is analyzed via thermogravimetric analysis (TGA) and with a dynamic gas sorption reactor (DGS). The DGS was designed and constructed by researchers within the Lubner Group, for the purpose of measuring CO_2 adsorption capacity and kinetics of adsorption in Mg_2(dobpdc) coated samples. The results show a negative correlation between polystyrene content in tetraamine appended Mg_2(dobpdc) based coatings and CO_2 uptake capacity under humid conditions.

TABLE OF CONTENTS

LIST OF FIGURES

1. Introduction

Since 1980 global atmospheric CO_2 concentrations have risen by almost 100 ppm[2] and are currently still rising. The presence of higher levels of CO_2 in the atmosphere has been found to cause significant increases in global temperature [3], which can be harmful to most of the world's ecosystems as well as human life. Predictions for reducing total global warming below 1.5 degrees Celsius before the end of the 21st century involve a reduction in the total amount of CO_2 produced annually but also rely on advancements in DAC technology to remove existing CO_2 from the atmosphere [4].

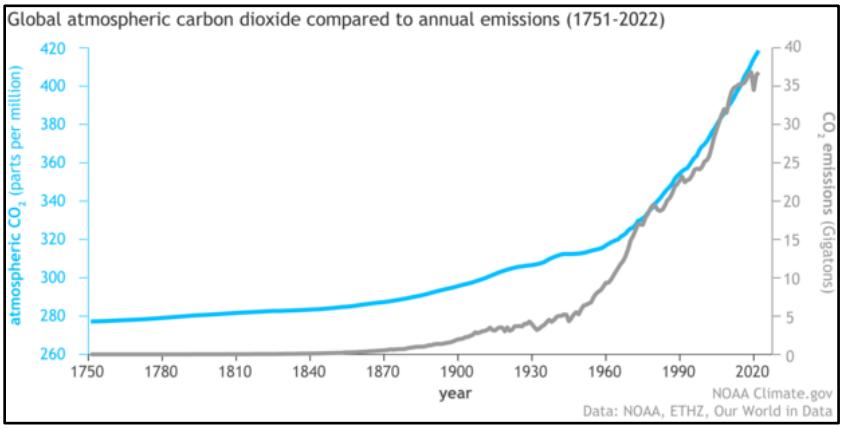

Figure 1. Global CO2 emissions and atmospheric concentrations [3][8]

Currently, DAC technology is limited both by its power requirements and its carbon capture efficacy, which makes DAC a cost-ineffective solution to reducing atmospheric CO_2 levels. Degradation of Mg2(dobpdc) in DAC systems constitutes an especially large portion of the cost associated with CO_2 capture, with the cost of kilogram sorbent per ton of CO_2 captured increasing as much as

150% over just three years of continuous operation [5]. Companies such as Climeworks currently operate commercially successful DAC sites that sequester CO_2 on the order of tens of thousands of tons CO_2 per year [6], but even with ideal conditions and local stores of geothermal energy, current costs are estimated at $\$600/tCO_2$ [7]. Furthermore, solid sorbent DAC (S-DAC) systems are relatively energy intensive, with typical S-DAC models requiring $9.5Gj/tCO_2$ [8] . Cheaper options exist, with some methods of carbon sequestration through forest growth costing less than $\$100/tCO_2$ [4] , but these methods take up large amounts of land that make implementation near major urban centers untenable [9].

To effectively limit global warming to the 1.5 degrees Celsius target set by the United Nations [10] DAC systems will need to be implemented alongside methods to reduce future CO_2 output. For DAC technologies to see widespread implementation, it is likely that the cost of CO_2 removal will need to be significantly decreased. One method of reducing the cost of CO_2 capture is by optimizing the sorbents used in S-DAC systems for maximum CO_2 capture efficiency. Currently DAC sorbent costs are the most variable cost in S-DAC systems ranging from \$10-140 per ton of CO_2 captured, making it difficult to create accurate economic models of S-DAC systems [11]. In this thesis, I address methods of improving and measuring the CO_2 adsorption properties of amine appended Mg2(dobpdc).

Amine Appended Mg2(dobpdc) has proven to be effective at capturing ambient CO_2 in the atmosphere, reaching concentrations as high as 5 mmol

CO_2/g MOF [12]. Mg2(dobpdc) selectively bonds with CO_2 molecules at the amine appended sites within the MOF leading to the formation of ammonium carbamate chains via chemisorption [13]. Mg2(dobpdc) can selectively bond with CO_2 while avoiding interaction with other gases due to precisely controlled pore sizes that are roughly the same diameter as CO_2 molecules [14] . Adsorption mechanism studies performed by the Long Group at UC Berkeley have found that Tetraamine appended Mg2(dobpdc) specifically allows for a theoretical maximum capacity of 2 CO_2 molecules per tetraamine. Experimental data obtained via TGA by the group found a CO_2 uptake capacity of roughly 3.6 mmol CO_2/g MOF in a pure CO_2 environment [15]. This CO_2 adsorption occurs within a relatively small range of temperatures and pressures, which allows for regeneration of the MOF via relatively small swings in temperature and pressure [12].

This MOF also demonstrates a resistance to oxidation, humidity as well as temperature and pressure swings when paired with a polystyrene binder [13]. This combination of characteristics make Mg2(dobpdc) particularly suitable for DAC applications as the sorbent can be used for several adsorption/desorption cycles without suffering a reduction in CO_2 capacity [16].

Without a binder, Mg2(dobpdc) is susceptible to degradation from humidity, which can reduce the surface area of the MOF, rendering it unable to absorb CO_2. Studies have found that the presence of a polymer binder, such as PDMS or polystyrene can prevent degradation of Mg2(dobpdc) [17]. It is currently

unknown; however, exactly how polystyrene additives affect the total CO_2 uptake capacity of Mg2(dobpdc). Tests using various weight fractions of MOF/Polymer coatings have been completed using styrene-butadiene-styrene (SBS) [18] and PDMS [17], but to date there are no studies measuring the relationship between polystyrene weight concentration and CO_2 uptake in MOF coatings.

Herein, we discuss methods of coating thin film PS/MOF solutions, as well as the impact of polystyrene on the adsorption kinetics of the coating.

2. Methods and Materials

2.1. Material Preparation

2.1.1. Synthesis of Magnesium-343 MOF crystals

The process of creating the MOF coatings used in this thesis began with the synthesis of magnesium-343 MOF (343-MOF). This process begins by dissolving 9.89g of H_4(dobpdc) in a mixture of 110 mL methanol and 90 mL N, N-dimetheylformamide (DMF), or volume ratio of 55:45. The mixture is then sonicated at room temperature in a closed vessel until the solution becomes transparent. 11.5g of $Mg(NO_3)2{\cdot}6H_2O$ is then placed in a 350mL high-pressure round bottom flask with a stir bar. The DMF/methanol solution is then filtered through a Buchner funnel into the magnesium salt to remove any undissolved ligand particles. The top of this new solution is then covered with parafilm and purged with argon for 25 minutes. The flask is then tightly sealed with a Teflon cap and placed in a glass dish filled with silicone oil and heated to 120 degrees Celsius overnight while stirring at 300 rpm.

After this process is completed, the solution is cooled to room temperature and vacuum filtered in a Buchner funnel to remove any liquid from the solution. The solid precipitate is then moved to a container with 300mL of DMF and stored at 60 degrees Celsius for 6 hours. The solution is then filtered once more, and the filtered liquid is disposed of. This process of filtering and re-storing the solution in DMF is then repeated two more times. Afterwards, the solution is filtered again in a Buchner funnel, and the filtered solid is moved to a container of methanol to be stored at 60 degrees Celsius for 6 hours. After storing is complete, the solution is filtered once again. This process of storing in methanol and then filtering is completed twice more to remove any residual DMF. Finally, the solid Mg2(dobpdc) is stored in methanol at room temperature until the MOF is used in the creation of coatings.

2.1.2. Amine Appending Magnesium -343 MOF (dobpdc):

After synthesis of the 343-MOF is complete, amines are then appended to the MOF. This process begins by dissolving 1g of spermine into 4g of toluene at 60 degrees Celsius. While the spermine is dissolving in toluene, stored Mg2(dobpdc) is vacuum filtered from methanol in a Buchner funnel. After filtering is complete, 150mg of Mg2(dobpdc) are added to the spermine and toluene solution and heated at 60 degrees Celsius for 12 hours. Afterwards, the appended MOF is vacuum filtered once again resulting in a dry product. The appended 343-MOF is then stored in a 20- or 40-mL vial with a Teflon cap.

2.1.3. Synthesis of 343-MOF Polystyrene Solution:

The 343-MOF and polystyrene coatings used in measuring CO_2 adsorption capacity are synthesized by combining solid polystyrene, toluene and amine appended 343-MOF. In this thesis, three separate coating solutions were synthesized at different concentrations of polystyrene. One solution each of 9%, 20% and 33% polystyrene by weight were created by weighing dry 343-MOF and solid polystyrene, then combining with toluene solvent at a ratio of 5 mL per 250mg dry MOF. The polystyrene weight fraction is determined only by the weight ratio of polystyrene and 343-MOF, so a 9% polystyrene solution would have 10mg polystyrene for every 100mg 343-MOF.

After each of the reagents are weighed, the 343-MOF, polystyrene and toluene are added to a 20mL vial with a stir bar placed inside. The vial is then sealed with a hard plastic cap and taped around the edges to prevent evaporation of toluene [19]. After the vial is sealed, it is placed on a magnetic agitator and left to stir for at least 6 hours to properly dissolve the polystyrene and disperse the 343-MOF throughout the solution.

2.1.4. Sample Manufacturing Through Coating Process:

The 343-MOF coatings used in this thesis were created by taking the liquid 343-MOF polystyrene solution and depositing it onto 6062 aluminum substrates of 10 by 30 mm. These substrates were cut to size using a water-jet cutter. After the aluminum substrates had been cut, each substrate was numbered and

weighed on an electronic analytical scale with a precision of 10 micrograms. The liquid solution was deposited onto the substrates via pipette at a volume of 400 microliters per sample.

Initial attempts utilized a PDMS mold to precisely control the volume and thickness of these coatings. Aluminum substrates were cut to specific dimensions and placed at the bottom of square PDMS molds 1 cm squared in area and 1 cm in height. The original intention of this method was to precisely control the geometry of the coated samples by taking advantage of the low surface energy of PDMS [20] to create a mold that would not bind to the liquid polystyrene compound. The geometry of the original molds was affected by the hydrophobic-hydrophobic interaction between PDMS and toluene [21] causing a phenomenon known as creep [22].

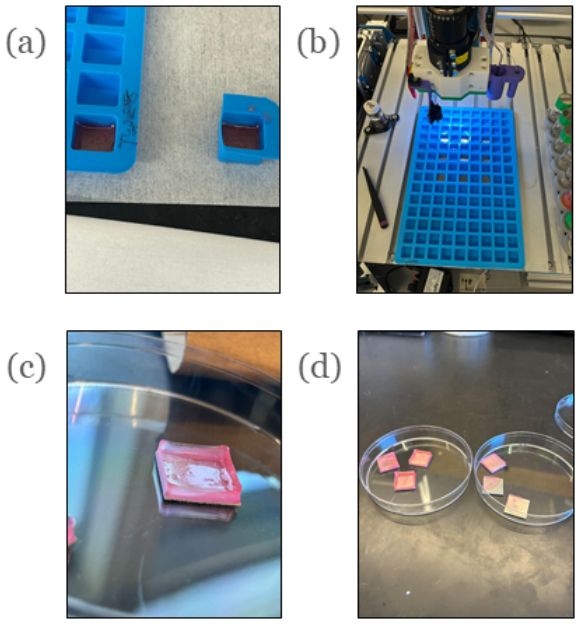

Figure 2. (a) & (b) Coating process for samples utilizing an automated pipette system to drop cast the MOF solution into a PDMS mold. (c) & (d) Samples retrieved from the PDMS mold exhibiting undesirable characteristics caused by creep.

Once the liquid had been deposited onto the substrate, a doctor blade was used to quickly spread the deposited solution into a uniform thickness. The height of the doctor blade was set to 800 micrometers, but the final thickness of the coatings was greatly reduced due to evaporation of the solvent. While not a perfectly smooth surface, the doctor blade is able to create a reasonably reproducible film coating [23].

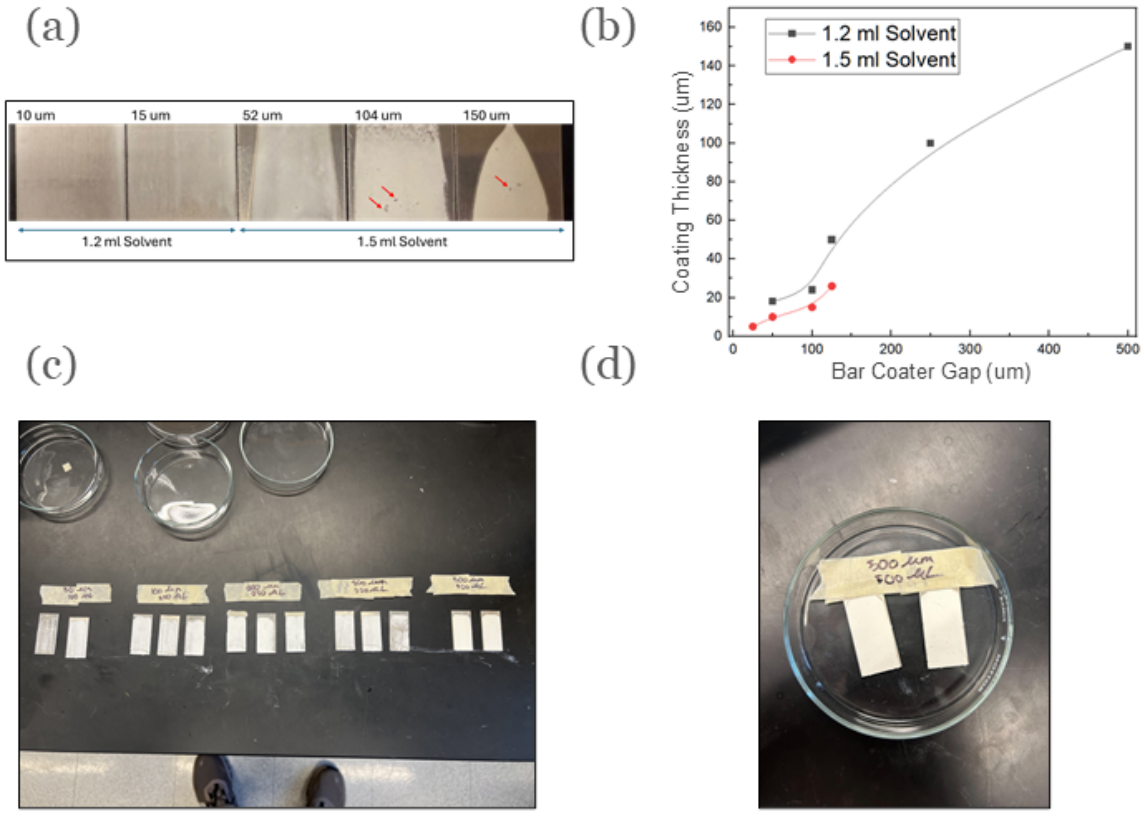

Figure 3. (a) & (b) Initial trials with doctor blade to confirm ideal film thickness. Doctor blade trail data is obtained from the Long Group, UC Berkeley. (c) & (d) Samples coated with the doctor blade on aluminum substrate.

After the coated samples had dried sufficiently, the samples were placed in a vacuum oven at 50 degrees Celsius and 200 mbar for at least 3 hours to ensure

any unevaporated toluene remaining in the samples was removed prior to testing [24]. It was imperative to remove any toluene or other volatile organic compounds (VOC) from the samples so as not to damage the LICOR sensor. Thermal degradation of the MOF or polystyrene does not occur in temperatures as low as 50 C. These samples were then left in open air inside the lab where testing was conducted for at least 24 hours to allow each sample to reach its maximum adsorbed CO_2 and H_2O capacity. Humidity varied slightly within the lab from roughly 40 to 62 percent, but CO_2 levels were constant at 400 ppm throughout the duration of the experiments.

2.2. Experimental Design

Typically, experiments measuring CO_2 adsorption capacity of various MOF classes are conducted via Thermogravimetric Analysis (TGA). In this thesis, the primary means of testing for CO_2 capacity was via DGS, with TGA measurements performed to validate the results of the DGS. One of the goals of this thesis is to utilize the DGS as a novel characterization method and to verify its accuracy against established characterization methods.

2.2.1. DGS Reactor Diagram:

The dynamic-gas sorption reactor (DGS) is a system built at Boston University through a collaboration between the Lubner group and the Werner group with the purpose of measuring CO_2 adsorption capacity of certain materials. The DGS consists of a kinetics chamber with Peltier element, one

ALICAT 10 standard cubic centimeter per-minute (SCCM) flow controller, one ALICAT 100 SCCM flow controller, a Chemglass AF-0513-20 bubbler, a BK Precision 9129B DC power supply and a LICOR LI-850 CO_2/H20 Sensor.

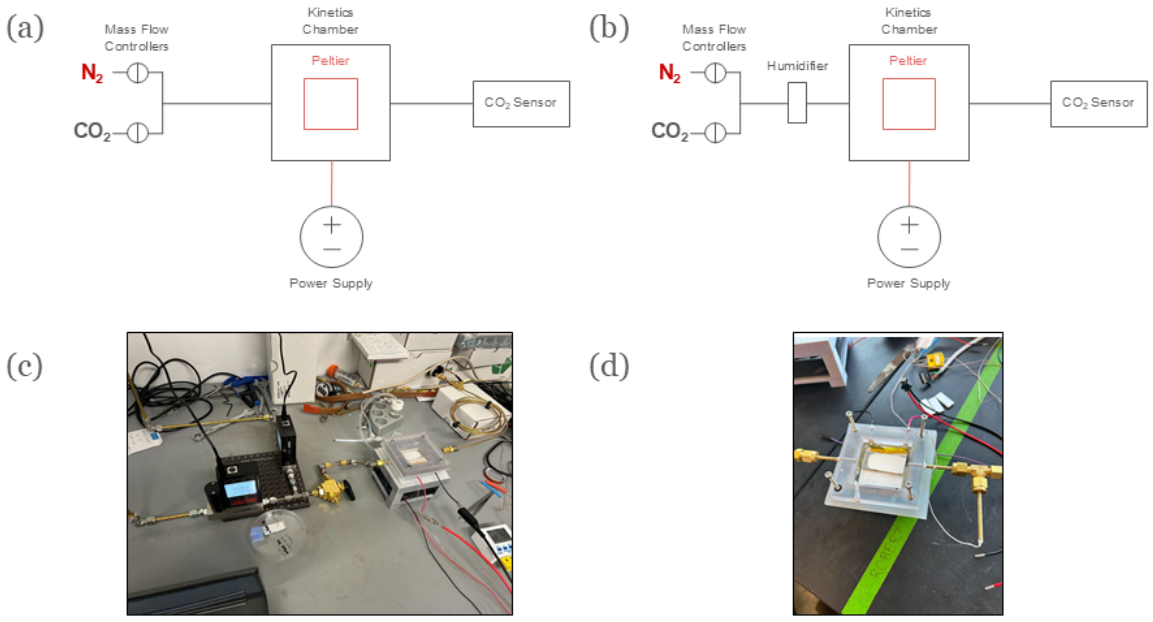

Figure 4. (a) DGS without humidifier for N_2 purge or CO_2 desorption. (b) DGS with humidifier attached for CO_2 Adsorption. (c) Image of the DGS kinetics chamber and mass flow controllers. Not pictured are the power supply, gas canisters, humidifier and CO_2 sensor. (d) Close up of the open kinetics chamber, with sorbent coated sample inside.

Two gas canisters, one filled with 5% CO_2 and 95% air and another with 100% N_2 gas are each connected to separate mass flow controllers. The CO_2 cylinder is connected to the 10 SCCM flow controller, while the N_2 cylinder is connected to the 100 SCCM flow controller. These mass flow controllers adjust the incoming flow rate of fluids to the kinetics chamber. The outlets of both mass flow controllers are connected via brass pipes sealed with Swagelock connectors.

This outlet pipe is then connected to the DGS chamber with flexible silicone tubing.

The kinetics chamber is composed of three polycarbonate layers separated by silicone sheets with inlet and outlet pipes, as well as a Peltier element and heat sink attached to the base. The DGS chamber is sealed via 4 machine screws that connect to a base made of polylactic acid (PLA). The PLA base also houses a computer fan beneath the chamber. The bottom layer of polycarbonate rests on an aluminum heat exchanger, with a Peltier element attached directly on top of the heat exchanger. Sorbent samples are placed directly on top of the Peltier element during experiments with the sorbent coated side facing upwards and the aluminum substrate in direct contact with the Peltier element. A wire thermocouple is placed onto the surface of the Peltier element with Kap-Ton tape and connected to a Supco SL500TC Thermocouple Temperature Data Logger. The positive and negative wires of the Peltier element are run through holes in the polycarbonate and sealed with Torr Seal. The Peltier element and fan are both connected to the power supply via jumper cables. The power supply supplies 8 volts and 2 amps of current to the Peltier element and the fan during the heating or cooling stages respectively. The inlet and outlet pipes are inserted via holes in the polycarbonate and sealed with Torr Seal. The outlet pipe is connected to the CO_2/H_2O sensor with flexible silicone tubing.

2.2.2. CO_2 Capacity Testing (DGS)

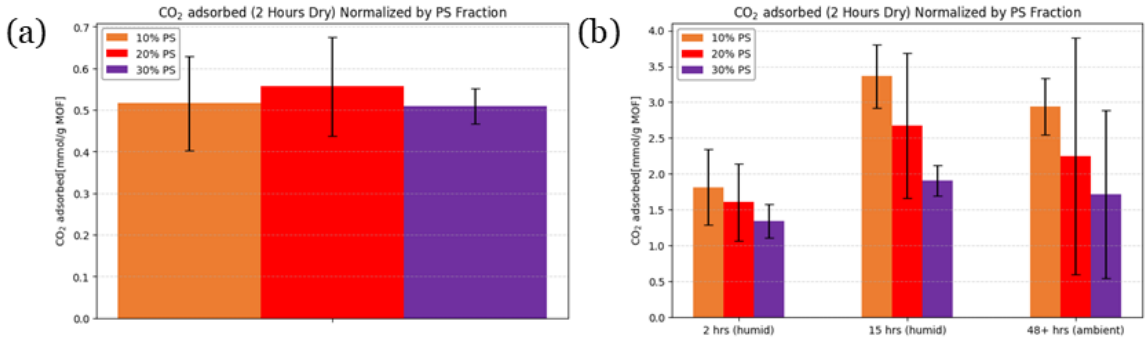

Figure 5. (a) Dry CO_2 adsorption capacity of various MOF/Polymer fraction coatings as measured by DGS. Error bars represent standard deviation in measured CO_2 uptake across multiple trials using the same sample. (b) Adsorbed humid CO_2 capacities at different adsorption times across 10, 20 and 30 percent polystyrene weight fraction MOF coatings. Error bars represent standard deviation in measured CO_2 uptake across multiple trials using different samples for each trial.

Experiments begin by placing the sample in the DGS kinetics chamber and sealing it. The chamber is then flushed with a concentration of 100 SCCM N_2 gas at ambient temperature until a ppm of 20 or less is recorded by the CO_2 sensor It has been determined experimentally in previous studies that CO_2 uptake of amine appended Mg_2(dobpdc) in a N_2 environment is negligible [25]. Once the Chamber has been flushed, the Peltier is activated and ramps up to a temperature of 120 degrees Celsius. This initiates the initial desorption cycle by removing most atmospherically adsorbed CO_2 from the sample. Once a concentration of 20 ppm is reached by the sensor, the Peltier element is powered off and a fan located beneath the reaction chamber is powered on to cool off the sample to 30 degrees Celsius.

Once this initial desorption and cooldown are completed, two adsorption cycles are conducted sequentially, one 2-hour long adsorption cycle and one 15-hour long adsorption cycle. In each cycle there are four phases: a CO_2 loading phase, an N_2 flushing phase, a CO_2 desorption phase and a cooldown phase. Before the CO_2 loading phase begins, a humidifier is added to the DGS in between the mass flow controllers and the reaction chamber. The addition of the humidifier takes place directly after the cooldown phase of the initial desorption. After the humidifier is added to the DGS, a nitrogen flushing phase is run until the CO_2 ppm is below 20 and the H20 mmol/mol is above 15. This step purges any latent CO_2 present in the humidifier and immediately precedes the CO_2 loading phase. Once these conditions are met, a CO_2 loading phase begins. During the CO_2 loading phase, the CO_2 mass flow controller is set to 10 SCCM while the N_2 mass flow controller is set to 90 SCCM, resulting in a gas mixture that is 5000 PPM CO_2, with N_2 as the remainder of the gas. This phase lasts for two hours after which the humidifier is removed. The CO_2 mass flow controller is reset to 0 SCCM and the N_2 mass flow controller is set to 100 SCCM to purge most residual H_2O and CO_2 in the chamber. Once the H_2O and CO_2 levels have been brought down to 5000 and 20 ppm respectively, the cycle is repeated exactly as stated before, but with a 15-hour adsorption cycle rather than 2 hours. Once all cycles have been completed, each sample will have gone through two adsorption cycles total.

2.2.3. CO_2 Capacity Measurements with TGA

Samples tested in the TGA consisted of dried and powdered MOF/Polymer solution placed in aluminum TGA pans. The TGA was used to measure differences in mass for an individual sample at a constant pressure. Temperature and gas composition inside the TGA chamber change depending on the current step of the trial. One sample was tested for each polymer weight fraction. Each sample was tested under the same conditions and followed the same testing procedure.

Tests begin by flushing the TGA chamber with pure N_2 at a flow rate of 20 ml/min starting at room temperature (30° C) for 5 minutes. Afterwards the flow and composition of the gases remain the same, but temperature gradually increased to 150° C over 1 hour. This temperature is then maintained for 3 hours to desorb any adsorbed CO_2 and H_2O present in the sample. The temperature then decreased over 1 hour to room temperature. Afterwards the sample is allowed to cool for 2 hours at room temperature. Once this time elapses, the gas composition is switched to pure CO_2 at an identical flow rate of 20 ml/min for 5 hours to allow for CO_2 adsorption in the sample.

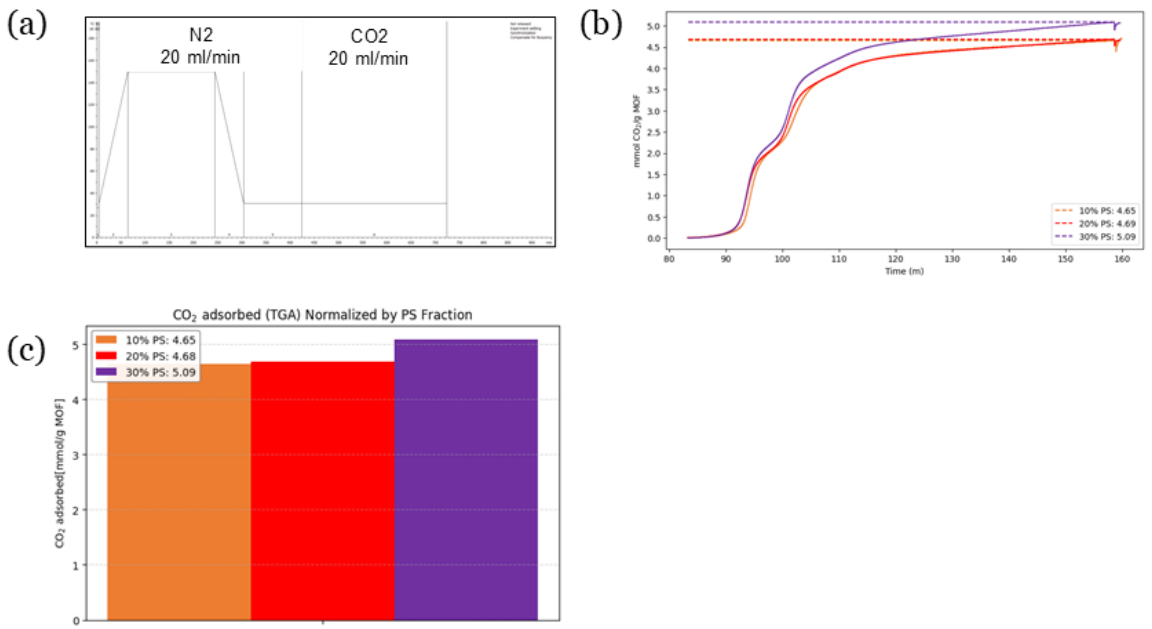

Figure 6. (a) Visual representation of the various stages of the desorption-adsorption cycle. (b) TGA sample weight during CO_2 adsorption normalized to dry weight of the sample. (c) CO_2 capacity per gram of sample across 10%, 20% and 30% polystyrene weight fraction samples as measured by TGA. TGA data is obtained from the Long Group, UC Berkeley.

Capacity of CO_2 per sample is then analyzed by taking the mass differential between the minimum mass recorded after cooling occurs, and the highest recorded mass during the adsorption cycle. It is expected that the lowest recorded mass of the sample represents the weight of the sample without any adsorbed foreign compounds. Similarly, it is expected that the additional mass present at the highest recorded mass reading is solely due to CO_2 adsorbed into the powdered material as no other gases are present in the chamber at the time of adsorption [26]. This mass differential is then normalized based on the weight of MOF estimated to be present in the sample used and converted to units of mmol CO_2/g MOF.

3. Results and Discussion

3.1. TGA

Dry CO_2 isobars were obtained via TGA of 343-MOF samples synthesized for this study at 10%, 20% and 30% polymer weight fractions. Of the samples analyzed, samples exhibited almost identical CO_2 uptake capacity regardless of polystyrene weight fraction. It is important to note that CO_2 adsorption measured in both TGA and DGS includes both chemisorbed and physisorbed CO_2. Uptake capacity of measured samples is also similar to those found in dry CO_2 isotherms as measured by the Jeff Long Group at UC Berkeley [27].

The almost identical uptake of CO_2 across a range of polystyrene weight fractions implies that the polystyrene binder used is actually not impacting the ability of Mg_2(dobpdc) to form ammonium carbamate bonds with CO_2. Previously it was believed that polystyrene could intercalate inside the pores of the Mg_2(dobpdc) crystals, thereby limiting the amount of carbon atoms that could bond to the amine appended MOF. If polystyrene chains can intercalate inside of the MOF pores, it doesn't seem to be impacting the overall capacity seen in the samples tested. The adsorption of CO_2 also seems to be approaching steady state, as can be seen in figure 6 (b), implying that the similar adsorption profiles of various polystyrene fraction samples are not due to errors caused by measuring adsorption far below the actual capacity of the samples.

3.2. DGS

Initial trials performed in this study measured CO_2 uptake over a relatively short timeframe (2 hours) and under dry conditions (less than 0.1% H_2O). After multiple trials were conducted, it was observed that the actual CO_2 adsorption of the compounds was significantly lower than their theoretical values should be according to studies performed on the same material by the Long Group at UC Berkeley [27].

Samples that underwent adsorption in dry conditions over 2 hours via DGS adsorbed almost exactly 0.5 mmol/g, regardless of the polystyrene weight fraction used in the coating.

These results show extremely diminished uptake capacity when compared to adsorption isobars obtained from prior studies. After some analysis, it was thought that the length of time allowed for CO_2 adsorption was simply insufficient, possibly due to the kinetics of the DGS chamber or the properties of the material itself. Trials were then conducted across the same range of polystyrene fractions at 15 hours in dry conditions and similar CO_2 capacities were obtained. Unlike the adsorption capacities obtained via TGA, these dry CO_2 capacities obtained via DGS were far below expected values and as such were considered to not be representative of the actual adsorption characteristics of these samples.

While the uptake capacity of the MOF samples was extremely reduced in dry conditions, it was observed that during the initial desorptions the samples underwent, capacity seemed to be relatively close to expected values from

literature. Since longer adsorption times had already been attempted under dry conditions with little increase in measured capacity, it was then hypothesized that humidity present in lab air was aiding adsorption of CO_2 in samples left out in ambient conditions [28].

To measure this hypothesis, the trials were then altered to observe CO_2 uptake capacity in humid conditions. After observing the uptake capacity of various samples in humid conditions it was found that not only was capacity greatly increased, but that the polystyrene weight fractions of the samples seemed to significantly impact uptake capacity.

As pictured above, adsorption is highest in samples with a low polystyrene weight fraction (9%) and decreases significantly as the weight fraction increases to 20%. Contrary to results obtained during dry CO_2 adsorption via DGS and TGA, the percentage of polystyrene in the MOF samples does seem to impact the amount of CO_2 adsorbed in the samples measured.

3.3. SEM

Scanning Electron Microscope (SEM) imagery shows notable changes to the macro and microstructure of the MOF samples as polystyrene weight fraction changes. Specifically, the 10% weight fraction coating exhibited large cracks in its macrostructure compared to 20% and 30% samples. The cracking shown is likely due to the reduced volume of polystyrene present in the coating, as the polystyrene acts as a binder connecting the MOF crystals together. Without sufficient quantities of this binder, the coating is more brittle and fragmented.

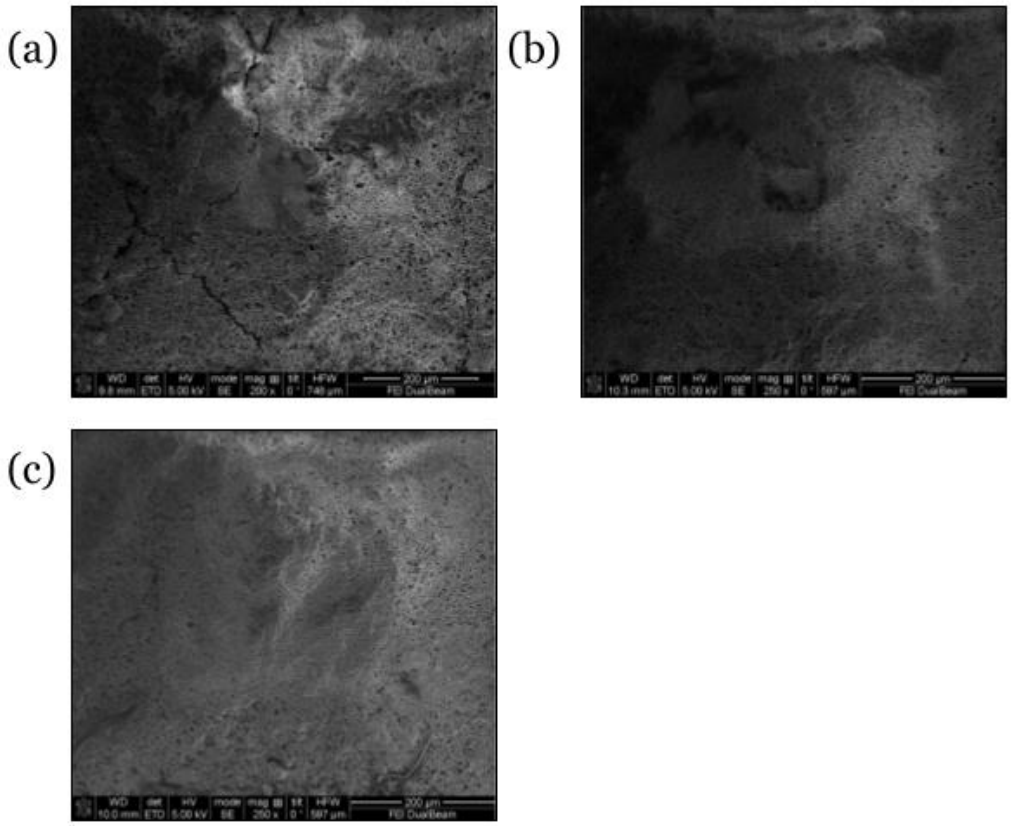

Figure 7. Scanning Electron Microscope (SEM) images of (a) 10%, (b) 20% and (c) 30% weight fraction MOF coatings.

Mechanical properties of these coatings have not been measured in this thesis, but it can be assumed that the formation of large cracks in the 10% polystyrene sample will lead to a mechanically weaker coating [29]. Thermal transport throughout the coating may also be inhibited due to gaps in between MOF crystals in the coating [30], making it difficult to achieve a more homogenous distribution of heat when desorbing CO_2 from the sample. One possible advantage of these disruptions in the macrostructure is an increase in the kinetics of CO_2 diffusion throughout the sample, although the most significant bottleneck in CO_2 adsorption is diffusion through the sorbent material itself [31].

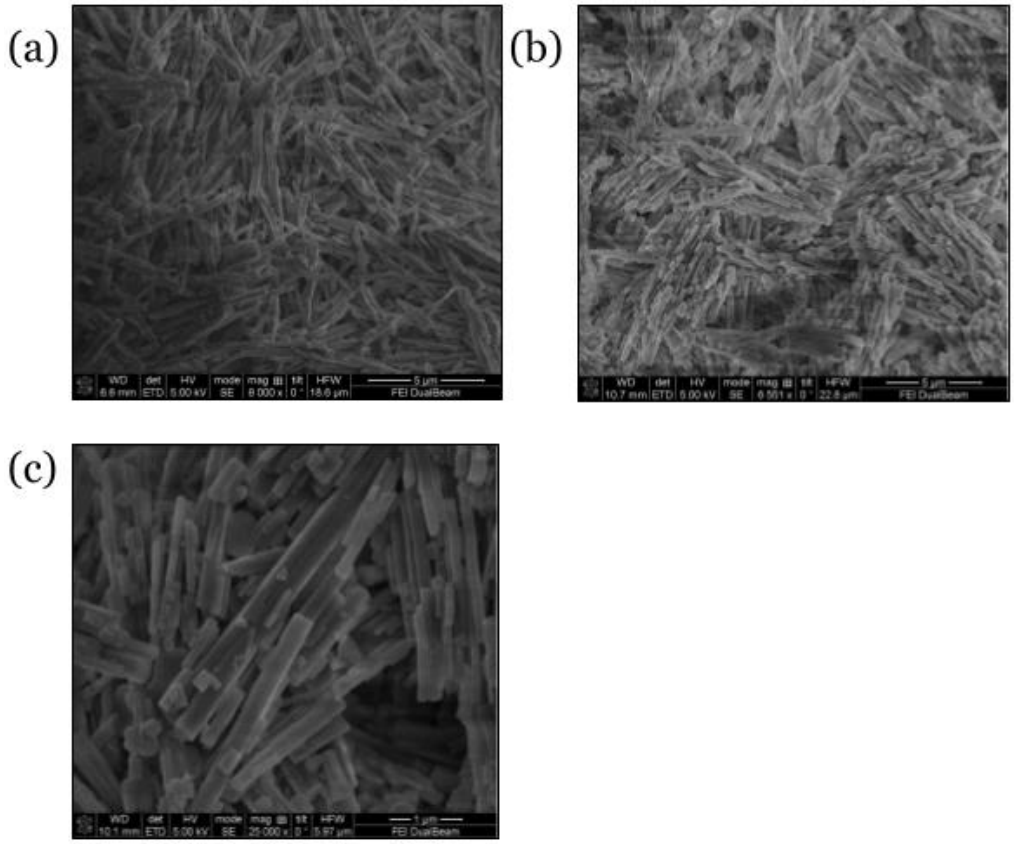

Figure 8. (a) SEM imagery from a 10% polystyrene sample. (b) SEM imagery from a 20% polystyrene sample. (c) SEM imagery from a 30% polystyrene sample.

Further magnification of the material showed minor differences in the amount of polystyrene present, but structurally the samples appeared to be very similar to each other. In some images, there appeared to be slightly more polystyrene present in the 30% sample, but these measurements are subjective and not quantifiable. The crystal size, structure and orientation remained unchanged across all samples measured. The consistency of crystal size and orientation implies that the quality of the samples themselves would not cause any changes to CO_2 adsorption capacity or adsorption speed.

4. Conclusion

4.1. Conclusion

The maximum recorded uptake of samples tested in this thesis was 5.09 mmol/g, while values confirmed by the Long Group showed maximum adsorption capabilities of roughly 5 mmol/g at the same temperature [27]. As shown in figure 6, increasing amounts of polystyrene in the MOF coatings do not seem to be correlated with a decrease in overall CO_2 capacity. While it was previously thought that polystyrene present in the coatings has the potential to physically block amine-appended adsorption sites within the MOF framework, TGA analysis now seems to suggest that polystyrene is instead limiting the mass transfer of H_2O which indirectly inhibits CO_2 uptake, slowing the formation of ammonium carbamate bonds. While H_2O has been shown to increase CO_2 uptake capacity in Mg_2(dobpdc), the presence of increasing amounts of polystyrene binder may slow the diffusion of H_2O, thereby slowing CO_2 adsorption rather than inhibiting it entirely.

Another possible explanation for the disagreement between TGA and DGS results is that the geometry of the coated samples used in DGS trials impacts the adsorption of CO_2. Samples used in the DGS trials consist of polystyrene/MOF solution that is drop coated onto aluminum samples at a set thickness of 850 micrometers. The samples used in TGA trials consist of polystyrene/MOF solution that is dried and powdered, forming individual particles of a non-standard size. The geometry of the DGS samples varies due to certain factors such as surface roughness, rate of evaporation etc. but could generally be modeled as a

thin sheet of coating with relatively consistent thickness. This geometry likely limits the diffusion of CO_2 through the adsorbent coating when compared to the powdered MOF solution used in TGA trials. Assuming the coated DGS samples are limited by the kinetics of diffusion of CO_2 through the coating, polystyrene may play a greater role in limiting diffusion of these samples than in limiting the diffusion of powdered TGA samples.

Based on results obtained in this study, it seems that polystyrene content slows the rate of diffusion of CO_2 through MOF coatings rather than stopping its adsorption entirely. This can be seen most prominently in the humid DGS trials, implying that polystyrene plays an important role in controlling the mass transfer of CO_2 while humidity is present. Furthermore, it seems highly likely that polystyrene or other hydrophobic binders may severely limit CO_2 uptake by preventing adsorption of H_2O.

4.2. Future works

There are several unanswered questions that have arisen throughout the writing of this thesis. The primary question that is still left unanswered is by what method polystyrene limits CO_2 uptake in tetraamine appended 343-MOF. The leading theory at the moment is that polystyrene chains dispersed in the MOF matrix physically prevent the diffusion of H_2O, thereby preventing the adsorption of CO_2 molecules.

Another unanswered question of interest is how various polystyrene weight fractions impact 343-MOF's ability to withstand degradation due to

humidity. Degradation mechanisms can vary between the MOF crystal structure or the amines appended to the crystal structure [14] and it is still unclear exactly which of these degradation mechanisms polystyrene binders have the potential to influence. Future studies could focus on the impact of thermal or humidity degradation in 343-MOF coatings by testing CO_2 capacity in samples across several humid adsorption/desorption cycles. Having a deeper understanding of how polystyrene can prevent degradation of MOF coatings is crucial to developing a full picture of CO_2 capture lifecycle analysis.

There is also potential for improving the studies conducted during this thesis by expanding on the range of polystyrene binders and developing a predictive model for CO_2 adsorption throughout this range of binders. To build a predictive model, it must be established whether the polystyrene binder forms a uniform conformal coating of the MOF crystals, or agglomerates heterogeneously. This could be determined by measuring the mass of a coated sample, then precisely measuring the sample's surface area to determine the required thickness for a conformal coating. For this to be possible, improvements would likely need to be made to the DGS system in order to ensure there are fewer sources of error in measurement. The DGS kinetics chamber in particular could be improved to reduce flow resistance of gases over the sample, which would decrease the potential for erroneous readings of CO_2 or H_2O. Similarly, improving control over the temperature of the gases used in the experiments as well as the temperature of the water in the humidifier would lead to improved

replicability in future experiments.

5. Acknowledgements

I am extremely grateful for the support of Dr. Lubner and my lab mates in the Lubner Group throughout the completion of this thesis. Over the last two years I've developed a passion for research through the collaboration and support of my peers which I hope to keep with me throughout my career. From the initial proposal of my thesis, I have received nothing but invaluable support and feedback from Dr. Lubner and the entire Lubner Group.

I would like to thank my committee members, Dr. Werner and Dr. Lubner for their time and advice throughout this challenging process.

I would also like to thank my parents for encouraging me to pursue a career in engineering and for their support and genuine interest in my studies. Despite not having a background in engineering themselves, they familiarized themselves with my topics of research to better understand my work.

Furthermore, I would like to thank my lab mates Hannes Albers, Corbyn Stosich, Mohammad Hadi and Savannah Schisler for their guidance throughout the completion of this thesis. Without the support of everyone involved, this project would not have been possible.

6. References

1. Ye, Z., Xie, Y., Kirlikovali, K. Architecting metal-organic frameworks at molecular level towards direct air capture, *Journal of the American Chemical Society*, 147(7), 5495–5514 (2025). https://doi.org/10.1021/jacs.4c12200
2. Lan, X., Tans, P. and K.W. Thoning: Trends in globally-averaged CO_2 determined from NOAA Global Monitoring Laboratory measurements. Version Friday, 05-Sep-2025 12:12:59 MDT https://doi.org/10.15138/9N0H-ZH07
3. Stips, A., Macias, D., Coughlan, C. *et al.* On the causal structure between CO_2 and global temperature. *Scientific Reports,* 6, 21691 (2016). https://doi.org/10.1038/srep21691
4. Rogelj, J., Luderer, G., Pietzcker, R. *et al.* Energy system transformations for limiting end-of-century warming to below 1.5 °C. *Nature Climate Change* 5, 519–527 (2015). https://doi.org/10.1038/nclimate2572
5. Habib Azarabadi, Klaus S. Lackner, A sorbent-focused techno-economic analysis of direct air capture, *Applied Energy*, 250, 959–975 (2019). https://doi.org/10.1016/j.apenergy.2019.04.012.
6. Climeworks switches on world's largest direct air capture plant. https://climeworks.com/press-release/climeworks-switches-on-worlds-largest-direct-air-capture-plant-mammoth
7. McQueen, N., Psarras, P., Pilorge, H., et al (2020). Cost Analysis of Direct Air Capture and Sequestration Coupled to Low-Carbon Thermal Energy in

the United States. *Environmental Science & Technology*, 54(12), 7542–7551 (2020). https://doi.org/10.1021/acs.est.0c00476

8. International Energy Agency. (n.d.). Direct Air Capture. https://www.iea.org/energy-system/carbon-capture-utilisation-and-storage/direct-air-capture
9. Chisholm PJ, Gray AN. Forest carbon sequestration on the west coast, USA: Role of species, productivity, and stockability. *PLoS One,* 19(5), e0302823 (2024). doi: 10.1371/journal.pone.0302823
10. United Nations. (2025). Goal 13: Take urgent action to combat climate change and its impacts. https://www.un.org/sustainabledevelopment/climate-change/
11. Sinha, A., Darunte, L., Jones, C., Systems Design and Economic Analysis of Direct Air Capture of CO_2 through Temperature Vacuum Swing Adsorption Using MIL-101(Cr)-PEI-800 and mmen-Mg2(dobpdc) MOF Adsorbents. *Industrial Engineering Chemistry Research*, 56(3), 750–764 (2017). https://doi.org/10.1021/acs.iecr.6b03887
12. Zhu Z, Tsai H, Parker ST, Lee JH, Yabuuchi Y, Jiang HZH, Wang Y, Xiong S, Forse AC, Dinakar B, Huang A, Dun C, Milner PJ, Smith A, Guimarães Martins P, Meihaus KR, Urban JJ, Reimer JA, Neaton JB, Long JR. High-Capacity, Cooperative CO_2 Capture in a Diamine-Appended Metal-Organic Framework through a Combined Chemisorptive and Physisorptive

Mechanism. *Journal of the American Chemical Society,* 146(9), 6072–6083 (2024). doi: 10.1021/jacs.3c13381

13. Hyun-Sik Moon, Jong-Ho Moon, Dong Hyuk Chun, Young Cheol Park, Yang No Yun, Muhammad Sohail, Kangkyun Baek, Hyunuk Kim, Synthesis of [Mg2(DOBDC)(DMF)2]@polystyrene composite and its carbon dioxide adsorption, *Microporous and Mesoporous Materials*, 232, 161–166 (2016). https://doi.org/10.1016/j.micromeso.2016.06.014
14. Xiaoyu Zhang, Hongshuo Zhao, Qian Yang, Mingshui Yao, Yi-nan Wu, Yifan Gu, Direct air capture of CO_2 in designed metal-organic frameworks at lab and pilot scale, *Carbon Capture Science & Technology*, 9, 100145 (2023). https://doi.org/10.1016/j.ccst.2023.100145
15. Eugene J. Kim *et al.*, Cooperative carbon capture and steam regeneration with tetraamine-appended metal–organic frameworks. *Science* 369(6502), 392–396 (2020). DOI:10.1126/science.abb3976
16. Darunte, L., Terada, Y., Murdock, C., Monolith-Supported Amine-Functionalized Mg2(dobpdc) Adsorbents for CO_2 Capture, *ACS Applied Materials & Interfaces*, 9(20), 17042–17050 (2017). https://doi.org/10.1021/acsami.7b02035
17. Yang, S., Karve, V., Justin, A., et. al (2021). Enhancing MOF performance through the introduction of polymer guests. *Coordination Chemistry Reviews,* 427, 213525 (2021). https://doi.org/10.1016/j.ccr.2020.213525

18. Yun Seok Chae, Sookyung Park, Dong Won Kang, Dae Won Kim, Minjung Kang, Doo San Choi, Jong Hyeak Choe, Chang Seop Hong, Moisture-tolerant diamine-appended metal–organic framework composites for effective indoor CO_2 capture through facile spray coating, *Chemical Engineering Journal*, 433(Part 3), 133856 (2022). https://doi.org/10.1016/j.cej.2021.133856

19. H. Yildirim Erbil, A. Yonca, (2002). Simultaneous Determination of Toluene Diffusion Coefficient in Air from Thin Tube Evaporation and Sessile Drop Evaporation on a Solid Surface. *Langmuir*, 18(13), 5113–5119 (2002). https://doi.org/10.1021/la011557a

20. Zheng, P., McCarthy, T. Rediscovering Silicones: Molecularly Smooth, Low Surface Energy, Unfilled, UV/Vis-Transparent, Extremely Cross-Linked, Thermally Stable, Hard, Elastic PDMS. *Langmuir*, 26(24), 18585–18590 (2010). https://doi.org/10.1021/la104065e

21. Guillerm, M., Couvert, A., Amrane, A. Characterization and selection of PDMS solvents for the absorption and biodegradation of hydrophobic VOCs. *Journal of Chemical Technology and Biotechnology*, 91(6), 1923–1927 (2016). https://doi.org/10.1002/jctb.4792

22. Ameli, N., Verma, J., Irungu, B.M. *et al.* Design and development of a novel polymer coating system with exceptional creep resistance. *npj Materials Sustainability,* 3, 21 (2025). https://doi.org/10.1038/s44296-025-00063-x

23. Butt, M. A. (2022). Thin-Film Coating Methods: A Successful Marriage of High-Quality and Cost-Effectiveness—A Brief Exploration. *Coatings*, 12(8), 1115. https://doi.org/10.3390/coatings12081115

24. Munday, E., Mullins, J., Edie, D. Vapor pressure data for toluene, 1-pentanol, 1-butanol, water, and 1-propanol and for the water and 1-propanol system from 273.15 to 323.15. *Journal of Chemical & Engineering Data*, 25(3), 191–194 (1980). https://doi.org/10.1021/je60086a006

25. Siegelman, R. L., McDonald, T. M., Gonzalez, M. I., Martell, J. D., Milner, P. J., Mason, J. A., Berger, A. H., Bhown, A. S., & Long, J. R. Controlling Cooperative CO_2 Adsorption in Diamine-Appended Mg_2(dobpdc) Metal-Organic Frameworks. *Journal of the American Chemical Society*, *139*(30), 10526–10538 (2017). https://doi.org/10.1021/jacs.7b05858

26. Mabokela, T., Somo, T., Maponya, T. Dynamic carbon dioxide uptake capacity of metal organic framework using thermogravimetrical evaluation at different CO2 pressure, *Materials Letters*, 317, 132086 (2022). https://doi.org/10.1016/j.matlet.2022.132086

27. Jarad A. Mason, Thomas M. McDonald, Tae-Hyun Bae, Jonathan E. Bachman, Kenji Sumida, Justin J. Dutton, Steven S. Kaye, and Jeffrey R. Long. Application of a High-Throughput Analyzer in Evaluating Solid Adsorbents for Post-Combustion Carbon Capture via Multicomponent

Adsorption of CO_2, N_2, and H_2O. *Journal of the American Chemical Society*, 137(14), 4787–4803 (2015). DOI: 10.1021/jacs.5b00838

28. Cammarere C, Cortés J, Glover TG, Snurr RQ, Hupp JT, Liu J. Water-enhanced CO2 capture in metal-organic frameworks. *Frontiers in Chemistry*, 13, 1634637 (2025). doi: 10.3389/fchem.2025.1634637

29. Awaja, F., Zhang, S., Tripathi, M. Cracks, microcracks and fracture in polymer structures: Formation, detection, autonomic repair. *Progress in Materials Science*, 83, 536–573 (2016). https://doi.org/10.1016/j.pmatsci.2016.07.007

30. Yun Long, Yuzhang Wang, Xiaohu Chen, Runxuan Sang, Influence of crack features on heat transfer characteristic and cracking behaviour of APS-YSZ coating: A numerical simulation study, *Ceramics International*, 47(15), 22209–22218 (2021). https://doi.org/10.1016/j.ceramint.2021.04.244.

31. Hou, C., Kumarb, D., Jinc, Y., et al. Porosity and hydrophilicity modulated quaternary ammonium-based sorbents for CO_2 capture. *Chemical Engineering Journal*, 413, 127532 (2021). https://doi.org/10.1016/j.cej.2020.127532

32. National Oceanic and Atmospheric Administration, CO2 emissions vs. concentrations 1751-2022, May 12, 2023. https://www.climate.gov/media/14596

7. Vita